

Comparison of Phosphor Removal Efficiency of Rain Treatment Materials Containing Illite

*¹Yootaek Kim, ²Taesung Chae

¹Department of Advanced Materials Eng., Kyonggi University, Suwon, 16227 Rep. of Korea

²Department of Advanced Materials Eng., Kyonggi University, Suwon, 16227 Rep. of Korea

*Corresponding author Email: ytkim@kgu.ac.kr

Abstract

Artificial lakes constitute more than 40% of drinking water sources, and can be easily eutrophicated by accumulation of phosphor, nitrogen, and nutrition salts introduced by various industrial and domestic origins after 10–30 years of their construction. Specifically, the concentration of phosphor is considered as an important factor that influences eutrophication, and causes seven times the eutrophication of nitrogen. In the present study, porous ceramics were fabricated with bottom ashes (BA) from power plants for recycling purposes and illite, which is known to be an efficient absorption material for phosphor in water. The phosphor removal efficiency reached up to 59% when the composition rate of illite to BA was 4 to 6. The study indicates the possibility of developing phosphor absorbing porous ceramics by using spent materials such as BA as substitutes for expensive illite without a significant decrease in phosphor removal efficiency.

Keywords: Phosphor removal, Rain treatment materials, Eutrophication, Porous ceramics, Illite, Bottom ash

1. Introduction

The total amount of artificial lakes with drinking water exceeds 40%, and these lakes are exposed to severe contamination from industrial and domestic sources 10–30 years after their construction. Eutrophication due to the increase in the concentration of nitrogen, phosphor, and nutrition salts causes a significant increase in the concentration of algae in the water [1, 2]. Previous studies reported that the concentration of phosphor is the most important factor when compared to other factors that influence eutrophication, and the effect of the phosphor concentration on eutrophication is seven times that of nitrogen [3]. Therefore, several studies examined methods to chemically, biologically, and physically remove phosphor in water in slow flowing or non-flowing areas [4].

Chemicals for water treatment were used to remove phosphor by creating insoluble or low soluble salt combined with phosphor. This chemical method is a popular method to remove phosphor. However, it is an expensive method, and also incurs additional costs for the removal of sludge produced during the precipitation reaction. The biological method uses microorganisms to remove phosphor in anaerobic conditions and extra-absorption in aerobic conditions. The biological method is a relatively simple process. However, the continuous removal of phosphor is difficult because microorganisms react sensitively with the surrounding environment and changes in pH. Physical methods that use absorbing materials involve a simple process, and are considered efficient, especially given a condition of low phosphor concentration, as well as easy control and maintenance [5].

Extant studies investigated absorption materials including aluminum oxide hydroxide, iron oxides, Fe–Mn binary oxide, a polymeric ligand exchanger, zirconium hydroxide as well as fly

ash and slags for economic reasons [6, 7]. Clay materials, such as kaolinite, montmorillonite, and illite, were examined for use as absorbers for phosphor. Previous studies reported that illite is the most efficient material for removing phosphor relative to various clay minerals [8]. Therefore, illite was used as the raw material, and bottom ashes from power plants were used for recycling and reducing the production cost of absorption materials. Spherical specimens with diameters of 8–10 mm were manufactured with a wide range of illite and BA contents. Specimens were sintered at a high temperature, and analyzed by various methods to estimate the possibility of applying the specimens to the absorbing material in the rain treatment system.

2. Materials and Methods

Illite is often termed as mica, fine mica, or mica clay mineral. It is formed from micas or feldspars by weathering, reaction with hot water, or by the process of attribute degeneration. Its chemical structure consists of a combination of tetrahedral layers and octahedral layers in a 2:1 proportion, and each unit layer is connected by K⁺ ions [9]. The illite used in the study was collected domestically and milled in a planetary ball mill (MTI Korea, SFM 1) at 400 rpm for 1 h. The mean diameter of milled illite was under 105 μm, and it was then used as a raw material without further sieving. Two colors, namely white and yellow, of illite powder were observed after milling. The color of illite may differ with respect to its composition as indicated in previous reports [9]. However, mixed powder was used in this study because differences were not observed in the XRD pattern analysis. The chemical components of illite were analyzed by XRF (Shimadzu EDX 720) and are shown in Table 1.

Fly ash (FA) produced from power plants as by-products is classified by the position of collection as FA and bottom ash (BA),

and the generation amount of BA is about 20%. In case of FA, over 80% is recycled as concrete mixture or raw material of cement. However, BA is rarely recycled, and only a small portion is recycled as bank or reclamation materials. Most unrecycled FA and BA were simply landfilled in ash ponds in power plants. Recently, there is an increase in the construction cost of ash pond because it is difficult to determine a suitable landfill area on

account of civil complaints by inhabitants near power plants and environment protection groups[10].

The BA used in the study was provided by a domestic (Y) power plant near a metropolitan area, and it was used as a raw material without any further processing. The chemical compositions of BA by XRF are also listed in Table 1

Table 1: Chemical composition of illite and bottom ash (BA).(wt. %)

	Ig. loss	SiO ₂	Al ₂ O ₃	Fe ₂ O ₃	CaO	MgO	Na ₂ O	K ₂ O	TiO ₂		Total
Illite	2.64	70.86	15.79	3.82	0.12	0.50	1.17	4.68	0.42		100.0
BA		61.31	21.35	9.81	3.54	1.08	0.60	1.25	1.06	0.11	100.0

Finely milled illite and BA were formed in spherically shaped specimens with a diameter range of 8 to 10 mm. The mixing ratios of illite to BA were in the range from 10:0 to 0:10 with two intervals, and are shown in the Table 2. The formed specimens were dried at 105 °C for 24 h, and then directly placed into a pre-heated furnace at room temperature. Subsequently, they were sintered at 1000 °C, 1100 °C, 1200 °C, and 1300 °C for 10 min.

Table 2: Proportion rate of raw materials in the specimens.(wt.%)

Specimen ratios	Illite	BA
10:0	100	0
8:2	80	20
6:4	60	40
4:6	40	60
2:8	20	80
0:10	0	100

The bulk density and water absorption rate of sintered specimens were measured by using the KS F 2503 method, and then surfaces and sliced surfaces were observed with an optical microscope (Sometch Vision S/V 2). The phosphor removal rates of the specimens were analyzed by XRD and IC (Ion-Chromatography; Dionex, ICS-2000). Additionally, 5 mg/L of KH₂PO₄ solution (SIGMA-ALDRICH, 778-77-0) was prepared to measure phosphor removal rates based on the reaction time. Subsequently, 0.1 N of NaOH was added to maintain the pH of the solution at 7. This is a general method to measure phosphor removal rates such that the ratio of solution to absorption materials (solids) is 1:20, and the amount of absorption materials is approximately 1 to 3 g[11].

In this study, 2 g of absorption material was placed in a beaker with 40 mL of phosphate solution, and then agitated by using an agitator (DAITHAN-Scientific, SMHS-3) at 250 rpm for 60 min to 720 min at 25 °C. Following the agitation, the solution was processed by a high-speed centrifuge machine (Haniil MF80 Centrifuge) at 3200 rpm for 4 min. After the centrifugal process, the upper solution was filtered by a 0.2 μm PTFE filter (WKPO 225-1), and the phosphate concentration was then analyzed by IC.

3. Results and Discussion

Figure 1 shows the bulk density and water absorption rate of the specimens measured by KS standard methods. The bulk density of porous ceramic specimens decreased with decrease in the illite content and sintering temperature. However, there was a significant decrease in the water absorption rate of the specimens

with increase in the sintering temperature from 1100 °C to 1300 °C. The illite and BA ratio of 6:4 and 0:10 specimens exhibited a significant decrease in water absorption between 1100 °C and 1300 °C.

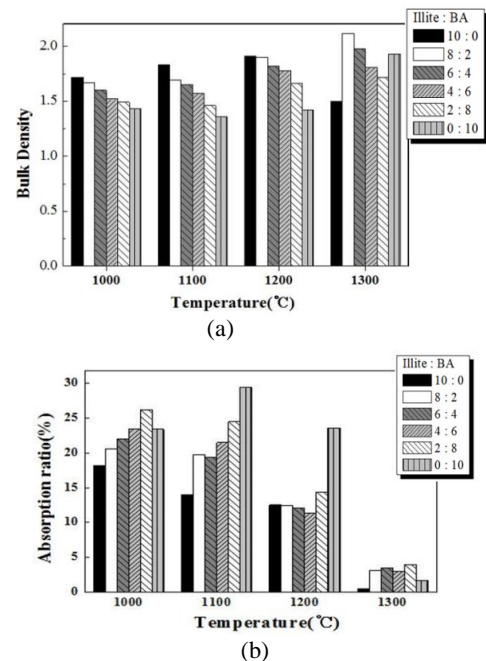
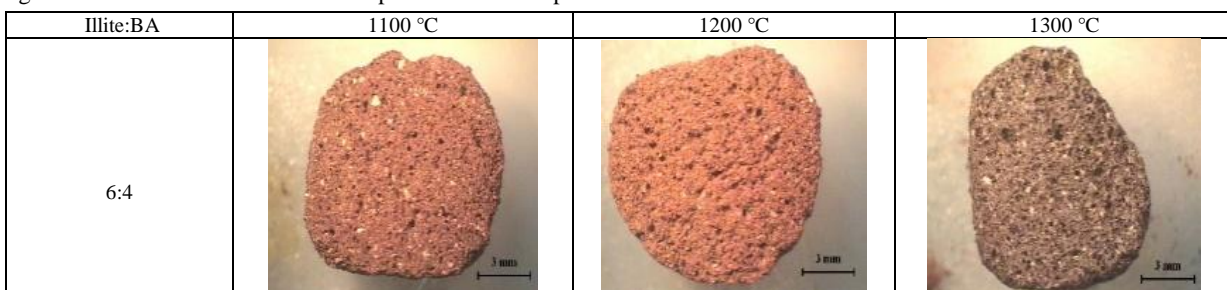


Figure 1: Bulk density and water absorption rate of specimens sintered at 1000 °C, 1100 °C, 1200 °C, and 1300 °C. (a) Bulk density and (b) Water absorption rate.

The cross-sectional specimens were observed by using an optical microscope to identify microstructural differences in specimens with different illite content ratios. Figure 2 shows the cross-sectional images of the specimens with two different illite contents and various sintering temperatures. It indicates that increasingly porous microstructures are observed in specimens with a higher content of illite and at higher sintering temperatures. The content ratio of illite and BA definitively affects the microstructures of the specimens. The increase in the illite content increases the porosity of the structure. The sharp decrease in the water absorption rate of the specimens sintered at between 1200 °C and 1300 °C is attributed to the formation of flux at the specimens sintered at 1300 °C irrespective of illite content.



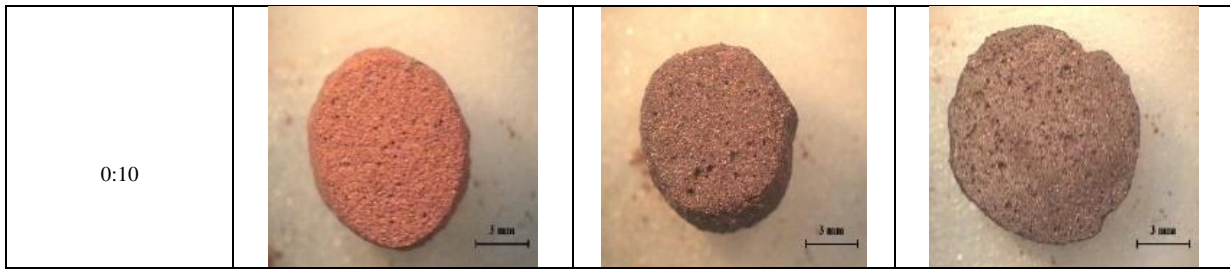


Figure 2: Optical cross-sectional micrographs (40 \times) of the specimens with different illite to BA ratios and sintering temperature. Increasingly porous microstructures are observed in specimens with higher illite content and at higher sintering temperatures.

Although it is necessary to identify the existence of flux by SEM (as shown in Figure 4) or other methods of microstructural observation, the flux is intuitively recognized by the color of the specimens that are considerably darker when compared with others. The existence of flux significantly decreases the water absorption rate of the specimens sintered at 1300 $^{\circ}\text{C}$ despite a slight change in bulk density at the same temperature range irrespective of illite content. The specimens were analyzed by XRD to investigate phase changes with variations in the ratio of illite to BA content.

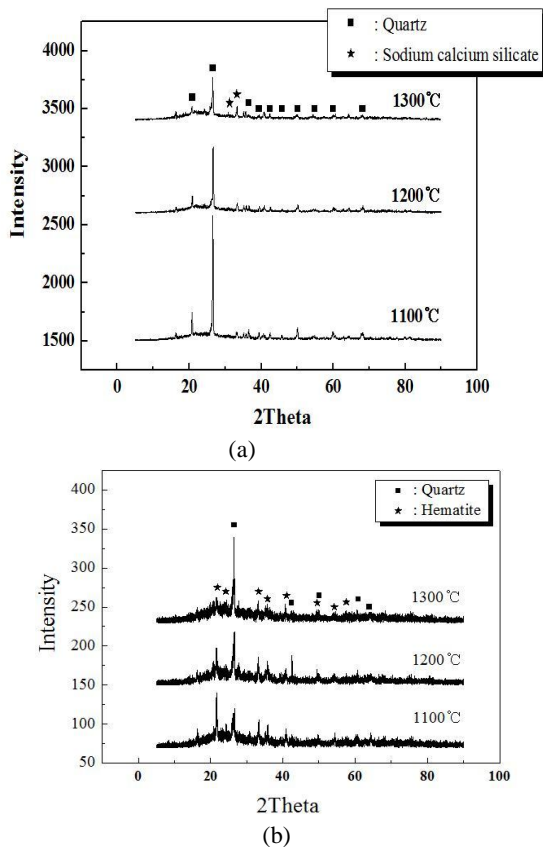


Figure 3: XRD patterns of specimens in Figure 2 with illite to BA ratios of (a) 6:4 and (b) 0:10.

As shown in Figure 3(a), the intensities of both quartz and sodium calcium silicate decreased with increase in sintering temperature, and this implies that the degree of crystallinity of the specimens decreased with increase in illite content and increase in sintering temperature when compared to the patterns and peaks in Figure 3(b). However, it is observed that even the crystallinity of the specimens sintered at 1300 $^{\circ}\text{C}$ is maintained higher than those in Figure 3(a). Conversely, quartz and hematite (Fe_2O_3) (expandable compound) phases are found in all the BA only specimens sintered above 1100 $^{\circ}\text{C}$ [11]. However, the peak intensities were low, and background intensities were high when compared to those of peaks in Figure 3(a). As shown in Figure 3(b), both the peak intensities of quartz and hematite increased with increases in the sintering temperature. This indicates that an increase in the

sintering temperature increases the quartz and hematite phases observed in the BA only specimens.

A sodium aluminum silicate ($\text{Al}_2\text{O}_3 \cdot \text{Na}_2\text{O} \cdot 6\text{SiO}_2$) phase appeared in the specimens containing illite in the ratio of 6:4 by forming a triclinic structure that displays the lowest degree of symmetry in the crystal system. Therefore, this indicates that the content of illite in the specimen can change the phases and the crystal structures of the specimen as well as the microstructures.

Generally, a liquid phase was formed on the surface of the specimen containing clay minerals if the sintering speed was excessively high and sintering temperature was sufficiently high. The liquid phase is termed as flux, and it fills the micro pores on the surface and causes the inside pore to close by blocking paths to the surface of the open pores [11]. Further details are given in Figure 4.

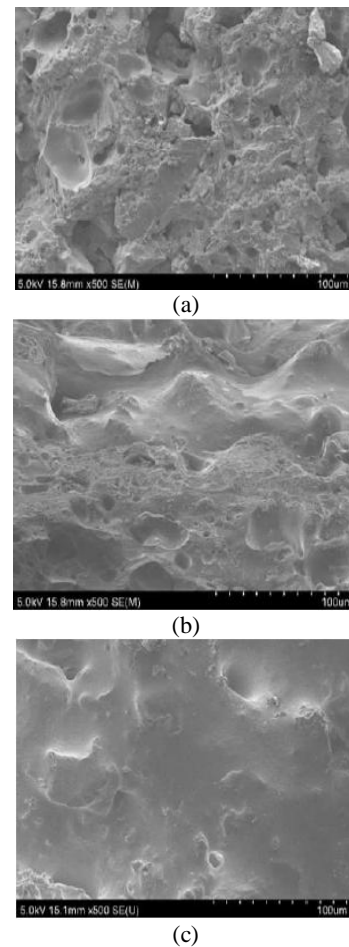


Figure 4: Cross-sectional SEM micrographs from three different specimens (a) BA only specimen sintered at 1200 $^{\circ}\text{C}$, (b) Specimen with illite to BA ratio of 6:4 sintered at 1200 $^{\circ}\text{C}$ and (c) Specimen with illite to BA ratio of 6:4 sintered at 1300 $^{\circ}\text{C}$.

As expected in the optical micrograph observation, a high amount of flux is observed on the surface of the specimen containing illite

sintered at 1300 °C as shown in Figure 4(c). Although a low amount of flux is also observed on the surface of the specimen containing illite sintered at 1200 °C, the flux amount is considerably lower than that of the specimen sintered at 1300 °C. The high amount of flux that appears at 1300 °C suggests a sharp decrease in the water absorption rate of the specimens sintered between 1200 °C and 1300 °C as previously mentioned, because the flux filled micro pores on the surface block the path to the surface of the open pores in the specimen.

In contrast, a flux phase is not observed in the specimens without illite contents as shown in Figure 4(a) owing to the high refractory property of BA. Flux was not observed for all specimens and at all sintering temperatures.

A reference solution of 5 mg/L was prepared by diluting 7.06 mg of KH_2PO_4 solution with distilled water. The concentration of phosphor in the solutions containing two specimens, namely the 100% illite only specimen and specimen with illite to BA ratio of 4:6, which were both sintered at 1200 °C, was measured by performing inductively coupled plasma (ICP) analysis after stirring the specimen solutions for 60 min and 720 min, respectively. The phosphor removal efficiencies of the illite only specimen and 60% BA containing specimens after stirring for 720 min were 60% and 59%, respectively, as shown in Figure 5.

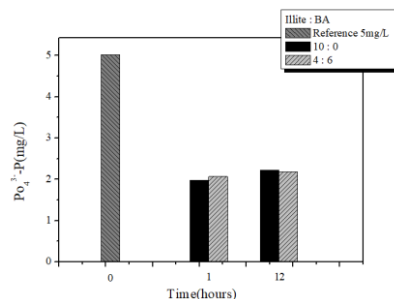


Figure 5: Concentration of phosphor before and after stirring for 1 h and 12 h (treatment) with absorbers. The concentrations of the reference solution (containing 5 mg/L phosphor) are shown in the leftmost bar in the figure.

The results indicated the absence of a relationship between the illite content of the specimen and phosphor removal rate. However, the phosphor removal rate of the specimen containing only 40% of illite is almost identical to or equivalent to that of the specimen composed of 100% illite. This result indicates that up to 60% of illite is replaced by recycled BA, and it reduces the production cost of the absorber for phosphor absorption.

4. Conclusion

The results indicate that it is possible to fabricate porous ceramics by using recycling materials such as BA up to 60%, and their phosphor removal efficiency is the same as or equivalent to that of the specimen composed of 100% illite. The ratio of illite in the specimen and agitation time is still the most important factors that influence the phosphor removal rate. However, BA substitutes illite up to 60% to fabricate porous ceramics as a phosphor absorber without any decrease in the phosphor removal rate.

Acknowledgment

This study was supported by a Kyonggi University Research Grant 2017.

References

- [1] Jung, W. H., & Kim G. H. (2006). Speciation of phosphorus dependent upon pH and oxidation reduction potential in overlying water and sediment: Journal of Korean Society of Environmental Engineers, 28(5), 472-479.
- [2] Park, S. J., Park, J. S., & Yoon, T. I. (2002). NOM removal and reduction of residual aluminum concentration by URC process and sand filter in eutrophicatedlake: Journal of Korean Society of Environmental Engineers, 24(3), 421-433.
- [3] Shin, G. W., Choo, Y. D., Kim, K. Y., Ryu, H. D., & Lee, S. I. (2011). Evaluation of Lanthanum(III) – loess composite as an adsorbent for phosphate removal: Journal of Korean Society of Environmental Engineers, 33(2), 143-148.
- [4] Zhao, D. Y., & Sengupta, Arup K. (1988). Ultimate removal of phosphate from wastewater using a new class of polymeric ion exchangers: Water Resource Research, 32(5), 1613-1625.
- [5] Cucarella, V., & Renman, G. (2009). Phosphorus sorption capacity of filter materials used for on-site wastewater treatment determined in batch experiments a comparative study: Journal of Environmental Quality, 38, 381-392.
- [6] Johansson, L. (1999). Industrial by-products and natural substrata as phosphorus sorbents: Environmental Technology, 20(3), 309-316.
- [7] Li, Y., Liu, C., Luan, Z., Peng, X., Zhu, C., Chen, Z., Zhang, Z., Fan, J., & Jia, Z. (2006). Phosphate removal from aqueous solutions using raw and activated red mud and fly ash: Journal of Hazardous Materials, 137(1), 374-383.
- [8] Choo, C. O., & Sung, I. H. (1999). A comparative study on adsorption behavior of heavy metal elements onto soil minerals: illite, halloysite, zeolite, and goethite: Journal of KoSES, 4(1), 57-68.
- [9] Cho, H. G., Park, O. H., Moon, D. H., Do, J. Y., & Kim, S. O. (2007). Phosphate adsorption of Young Dong illite: Journal of Mineralogical Society of Korea, 20(4), 327-337.
- [10] Duk, K. K., Kim, J. W., Kim, Y. T., Kang, S. G., & Lee, K. G. (2010). Production of lightweight aggregates using power plant reclaimed ash: Journal of the Korean Ceramic Society, 47(6), 583-589.
- [11] Kim, D. S., Lee, C. K., & Park, J. H. (2002). Sintering properties of artificial lightweight aggregate prepared from coal ash and limestone: Journal of the Korean Ceramic Society, 39(3), 259-264.